PHYSICAL REVIEW D **96,** 115007 (2017)

COHERENT enlightenment of the neutrino dark side

Pilar Coloma,[1,*] M. C. Gonzalez-Garcia,[2,3,4,†] Michele Maltoni,[5,‡] and Thomas Schwetz[6,§]

[1]*Theory Department, Fermi National Accelerator Laboratory, P.O. Box 500, Batavia, Illinois 60510, USA*
[2]*C.N. Yang Institute for Theoretical Physics, Stony Brook University, Stony Brook, New York 11794-3840, USA*
[3]*Departament de Fisíca Quàntica i Astrofísica and Institut de Ciencies del Cosmos, Universitat de Barcelona, Diagonal 647, E-08028 Barcelona, Spain*
[4]*Institució Catalana de Recerca i Estudis Avançats (ICREA), Pg. Lluis Companys 23, 08010 Barcelona, Spain*
[5]*Instituto de Física Teórica UAM/CSIC, Calle de Nicolás Cabrera 13–15, Universidad Autónoma de Madrid, Cantoblanco, E-28049 Madrid, Spain*
[6]*Institut für Kernphysik, Karlsruher Institut für Technologie (KIT), D-76021 Karlsruhe, Germany*

(Received 19 August 2017; published 11 December 2017)

In the presence of nonstandard neutrino interactions (NSI), oscillation data are affected by a degeneracy which allows the solar mixing angle to be in the second octant (also known as the dark side) and implies a sign flip of the atmospheric mass-squared difference. This leads to an ambiguity in the determination of the ordering of neutrino masses, one of the main goals of the current and future experimental neutrino program. We show that the recent observation of coherent neutrino-nucleus scattering by the COHERENT experiment, in combination with global oscillation data, excludes the NSI degeneracy at the 3.1σ (3.6σ) C.L. for NSI with up (down) quarks.

DOI: 10.1103/PhysRevD.96.115007

I. INTRODUCTION

The standard three-flavor oscillation scenario is supported by a large amount of data from neutrino oscillation experiments. The determination of oscillation parameters (see, e.g., Ref. [1]) is very robust, and for a broad range of new physics scenarios, only small perturbations of the standard oscillation picture are allowed by data. There is, however, an exception to this statement: in the presence of nonstandard neutrino interactions (NSI) [2–4], a degeneracy exists in oscillation data, leading to a qualitative change of the lepton mixing pattern. This was first observed in the context of solar neutrinos, where for suitable NSI the data can be explained by a mixing angle θ_{12} in the second octant, the so-called large mixing angle-Dark (LMA-D) [5] solution. This is in sharp contrast to the established standard Mikheyev-Smirnov-Wolfenstein (MSW) solution [2,6], which requires a mixing angle θ_{12} in the first octant.

The origin of the LMA-D solution is a degeneracy in oscillation probabilities due to a symmetry of the Hamiltonian describing neutrino evolution in the presence of NSI [7–10]. This degeneracy involves not only the octant of θ_{12} but also a change in sign of the larger neutrino mass-squared difference, $\Delta m^2{}_{31}$, which is used to parametrize the type of neutrino mass ordering (normal versus inverted). Hence, the LMA-D degeneracy makes it impossible to determine the neutrino mass ordering by oscillation experiments [10] and therefore jeopardizes one of the main goals of the upcoming neutrino oscillation program. As discussed in Refs. [5,10–12], nonoscillation data (such as that from neutrino scattering experiments) is needed to break this degeneracy.

Recently, coherent neutrino-nucleus scattering [13] has been observed for the first time by the COHERENT experiment [14], using neutrinos produced at the Spallation Neutron Source (SNS) at Oak Ridge National Laboratory. The potential of neutrino-nucleus scattering for constraining NSI has been studied, e.g., in Refs. [11,15–19]. The observed interaction rate at COHERENT is in good agreement with the Standard Model (SM) prediction. In this work, we show that this result excludes the LMA-D solution at 3.1σ (3.6σ) C.L. for NSI with up (down) quarks when combined with oscillation data.

II. NSI FORMALISM AND THE LMA-D DEGENERACY

We consider the presence of neutral-current (NC) NSI in the form of dimension-6 four-fermion operators, following the notation of Ref. [8]. Since we are interested in the contribution of the NSI to the effective potential of neutrinos in matter, we will only consider vector interactions in the form

$$\mathcal{L}_{\rm NSI} = -2\sqrt{2}G_F\epsilon^{f,V}_{\alpha\beta}(\bar{\nu}_{\alpha L}\gamma^\mu\nu_{\beta L})(\bar{f}\gamma_\mu f), \qquad (1)$$

*pcoloma@fnal.gov
†maria.gonzalez-garcia@stonybrook.edu
‡michele.maltoni@csic.es
§schwetz@kit.edu

where $\alpha, \beta = e, \mu, \tau$, and f denotes a SM fermion. The parameter $\epsilon^{f,V}_{\alpha\beta}$ parametrizes the strength of the new interaction relative to the Fermi constant G_F, and Hermiticity requires that $\epsilon^{f,V}_{\alpha\beta} = (\epsilon^{f,V}_{\beta\alpha})^*$. In gauge invariant models of new physics at high energies, NSI parameters are expected to be subject to tight constraints from charged lepton observables [20,21], leading to no visible effect in oscillations. However, more recently, it has been argued that viable gauge models with light mediators (i.e., below the electroweak scale) may lead to observable effects in oscillations without entering in conflict with other bounds [22–24] (see also Ref. [25] for a discussion). In particular, for light mediators, bounds from high-energy neutrino scattering experiments such as CHARM [26] and NuTeV [27] do not apply. In this framework, prior to the COHERENT results, the only direct bounds on NC NSI with quarks arise from their effect on neutrino oscillations when propagating in matter (for bounds in the heavy mediator case, see Ref. [11]). In the following, we will assume that the mediator responsible for the NSI has a mass larger than about 10 MeV, and hence the contact interaction approximation adopted in Eq. (1) applies for COHERENT.

The operators in Eq. (1) will contribute to the effective matter potential in the Hamiltonian describing the evolution of the neutrino flavor state,

$$H_{\rm mat} = \sqrt{2} G_F N_e(x) \begin{pmatrix} 1+\epsilon_{ee} & \epsilon_{e\mu} & \epsilon_{e\tau} \\ \epsilon^*_{e\mu} & \epsilon_{\mu\mu} & \epsilon_{\mu\tau} \\ \epsilon^*_{e\tau} & \epsilon^*_{\mu\tau} & \epsilon_{\tau\tau} \end{pmatrix}, \quad (2)$$

$$\epsilon_{\alpha\beta}(x) = \sum_{f=e,u,d} Y_f(x) \epsilon^{f,V}_{\alpha\beta}, \quad (3)$$

with $Y_f(x) \equiv N_f(x)/N_e(x)$, $N_f(x)$ being the density of fermion f along the neutrino path. Therefore, the effective NSI parameters entering oscillations, $\epsilon_{\alpha\beta}$, may depend on x and will be generally different for neutrinos crossing the Earth or the solar medium. The "1" in the ee entry in Eq. (2) corresponds to the standard matter potential [2,6]. In this work, we consider the cases of NSI with either up ($f = u$) or down ($f = d$) quarks. Note that oscillation experiments are only sensitive to differences between the diagonal terms in the matter potential (for instance, $\epsilon_{ee} - \epsilon_{\mu\mu}$ and $\epsilon_{\tau\tau} - \epsilon_{\mu\mu}$).

In general, neutrino evolution is invariant if the relevant Hamiltonian is transformed as $H \to -H^*$. This is a consequence of the CPT symmetry; see Refs. [7,8] for a discussion in the context of NSI. In vacuum, this transformation can be realized by changing the oscillation parameters as

$$\begin{aligned} \Delta m^2_{31} &\to -\Delta m^2_{31} + \Delta m^2_{21} = -\Delta m^2_{32}, \\ \sin\theta_{12} &\leftrightarrow \cos\theta_{12}, \\ \delta &\to \pi - \delta, \end{aligned} \quad (4)$$

where δ is the leptonic Dirac CP phase, and we are using here the parametrization conventions from Ref. [10]. The symmetry is broken by the standard matter effect, which allows a determination of the octant of θ_{12} and (in principle) of the sign of $\Delta m^2{}_{31}$. However, in the presence of NSI, the symmetry can be restored if in addition to the transformation Eq. (4) NSI parameters are transformed as [8–10]

$$\begin{aligned} (\epsilon_{ee} - \epsilon_{\mu\mu}) &\to -(\epsilon_{ee} - \epsilon_{\mu\mu}) - 2, \\ (\epsilon_{\tau\tau} - \epsilon_{\mu\mu}) &\to -(\epsilon_{\tau\tau} - \epsilon_{\mu\mu}), \\ \epsilon_{\alpha\beta} &\to -\epsilon^*_{\alpha\beta} \qquad (\alpha \neq \beta). \end{aligned} \quad (5)$$

Equation (4) shows that this degeneracy implies a change in the octant of θ_{12} (as manifest in the LMA-D fit to solar neutrino data [5]) as well as a change in the neutrino mass ordering, i.e., the sign of $\Delta m^2{}_{31}$. For that reason, it has been called "generalized mass ordering degeneracy" in Ref. [10].

The $\epsilon_{\alpha\beta}$ in Eq. (5) are defined in Eq. (3) and depend on the density and composition of the medium. It is easy to see that, if NSI simultaneously affect both up and down quarks with a coupling proportionally to their charge, $\epsilon^{u,V}_{\alpha\beta} = -2\epsilon^{d,V}_{\alpha\beta}$, the dependence on x cancels out for neutral matter and the degeneracy is mathematically exact. In this work, however, we consider only NSI with either up or down quarks, and hence the degeneracy will be approximate, mostly due to the nontrivial neutron density along the neutrino path inside the Sun [8].

III. GLOBAL FIT TO OSCILLATION DATA

For oscillation constraints on NSI parameters and the detailed description of methodology and data included, we refer to the comprehensive global fit in the framework of 3-flavor oscillations plus NSI with up and down quarks performed in Ref. [8]. In principle, the analysis depends on six oscillations parameters plus eight NSI parameters per f target, of which five are real and three are phases. To keep the fit manageable in Ref. [8], only real NSI were considered, and $\Delta m^2{}_{21}$ effects were neglected in the analysis of atmospheric and long-baseline experiments. This renders the analysis independent of the CP phase in the leptonic mixing matrix. For further details, see Ref. [8]. For completeness, we show the results of this fit as dashed lines in Fig. 1. Two different sets of solutions are shown: dashed blue lines corresponding to the LMA solution and dashed red lines corresponding to the LMA-D solution, which implies a flipped mass spectrum and θ_{12} in the second octant according to Eq. (4).

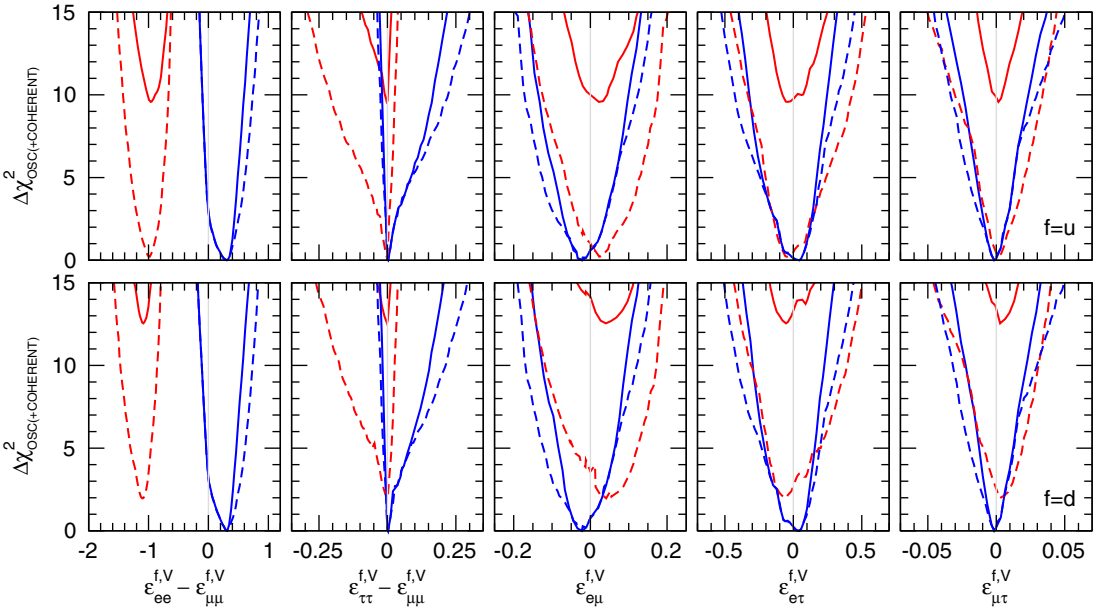

FIG. 1. $\Delta\chi^2$ as a function of NSI parameters $\epsilon^{f,V}_{\alpha\beta}$, for a global fit to oscillation experiments (dashed curves) and for a fit to oscillations and COHERENT data (solid curves). Blue lines correspond to the LMA solution ($\theta_{12} < \pi/4$), while the red lines correspond to the LMA-D solution ($\theta_{12} > \pi/4$). We minimize the χ^2 with respect to all oscillations parameters and all undisplayed NSI parameters in each panel.

IV. COHERENT RESULTS

The COHERENT Collaboration has recently reported the observation of coherent neutrino-nucleus scattering at 6.7σ [14]. The experiment uses neutrinos produced from pion decay at rest and a 14.6 kg CsI[Na] detector. Here, we describe our implementation of their constraints on NSI parameters, following closely Ref. [14].

At the SNS, the neutrino flux consists of a monochromatic ν_μ line coming from $\pi^+ \to \mu^+\nu_\mu$, plus a continuous spectrum of $\bar{\nu}_\mu$ and ν_e from the subsequent μ^+ decay. Hence, the total number of coherent scattering events will receive contributions from the three flux components, ν_μ, $\bar{\nu}_\mu$, and ν_e. We extract the relative contribution f_α of each flavor to the total number of events from the shaded histograms of Fig. S11 in the supplementary material of Ref. [14] as $f_{\nu_e} = 0.31$, $f_{\nu_\mu} = 0.19$, and $f_{\bar{\nu}_\mu} = 0.50$. Coherent elastic neutrino-nucleus interactions take place with a momentum transfer $Q^2 \simeq 2ME_r$, where E_r is the recoil energy of the nucleus and M is its mass. Thus, for the COHERENT experiment, the contact interaction approximation is valid for interactions with mediator masses above 10 MeV [11]. Within this approximation, for neutrinos of flavor α interacting with a nucleus with total zero spin, for which both the sum of proton spins and of neutron spins is also zero, the interaction rate is sensitive to the following combination of SM and NSI vector couplings (see, e.g., Ref. [15]):

$$Q^2_{w\alpha} \propto [Z(g^V_p + 2\epsilon^{u,V}_{\alpha\alpha} + \epsilon^{d,V}_{\alpha\alpha}) + N(g^V_n + \epsilon^{u,V}_{\alpha\alpha} + 2\epsilon^{d,V}_{\alpha\alpha})]^2 + \sum_{\beta\neq\alpha}[Z(2\epsilon^{u,V}_{\alpha\beta} + \epsilon^{d,V}_{\alpha\beta}) + N(\epsilon^{u,V}_{\alpha\beta} + 2\epsilon^{d,V}_{\alpha\beta})]^2. \quad (6)$$

Here, N and Z are the number of neutrons and protons in the target nucleus (we take into account the contributions from both Cs and I), and $g^V_p = 1/2 - 2\sin^2\theta_W$ and $g^V_n = -1/2$ are the SM couplings of the Z boson to protons and neutrons, respectively, θ_W being the weak mixing angle. The predicted number of signal events $N_{\rm NSI}$, for a given set of NSI parameters ε, can be expressed as

$$N_{\rm NSI}(\varepsilon) = \gamma[f_e Q^2_{we}(\varepsilon) + (f_{\nu_\mu} + f_{\bar{\nu}_\mu})Q^2_{w\mu}(\varepsilon)], \quad (7)$$

where γ is an overall normalization constant which depends on the exposure, detector efficiencies, etc. We then construct a chi-squared function $\chi^2_{\rm COH}$ using just the total number of events, according to the expression given in the supplementary material of Ref. [14]. We consider $N_{\rm meas} = 142$ observed events and take into account the statistical errors of the signal and the subtracted background, as well as systematic errors of the signal (28%) and beam-on background (25%). The normalization constant γ (whose value is not provided in Ref. [14]) is determined by requiring the χ^2 to be zero at the best-fit point quoted in Ref. [14] (i.e., $\epsilon^{u,V}_{ee} = -0.57$, $\epsilon^{d,V}_{ee} = 0.59$, all other $\epsilon^{f,V}_{\alpha\beta} = 0$).[1]

To illustrate the impact of COHERENT on the LMA-D solution, we show in Fig. 2 the chi squared for oscillations and for the COHERENT experiment separately, projected onto the $\epsilon^{f,V}_{ee}$ versus $\epsilon^{f,V}_{\mu\mu}$ plane. In this example, we have

[1]Let us note that, with this procedure, our constraints on $\epsilon^{u,V}_{ee}$ and $\epsilon^{d,V}_{ee}$ turn out slightly weaker than the result in Ref. [14] (our 90% C.L. interval is about 20% larger). Hence, our results can be regarded as conservative.

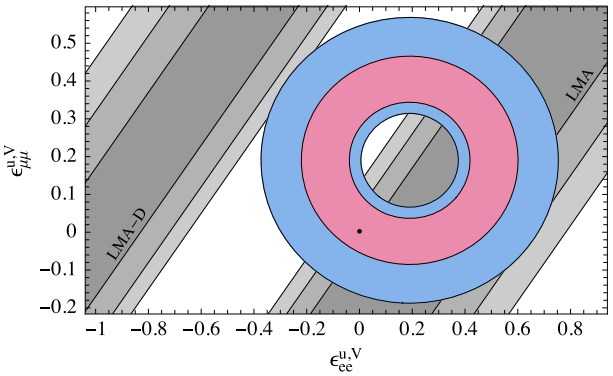

FIG. 2. Allowed regions in the plane of $\epsilon^{u,V}_{ee}$ and $\epsilon^{u,V}_{\mu\mu}$ from the COHERENT experiment shown together with the allowed regions from the global oscillation analysis. Diagonal shaded bands correspond to the LMA and LMA-D regions as indicated, at 1σ, 2σ, 3σ [2 degrees of freedom (dof)]. The COHERENT regions are shown at 1σ and 2σ only because the 3σ region extends beyond the boundaries of the figure.

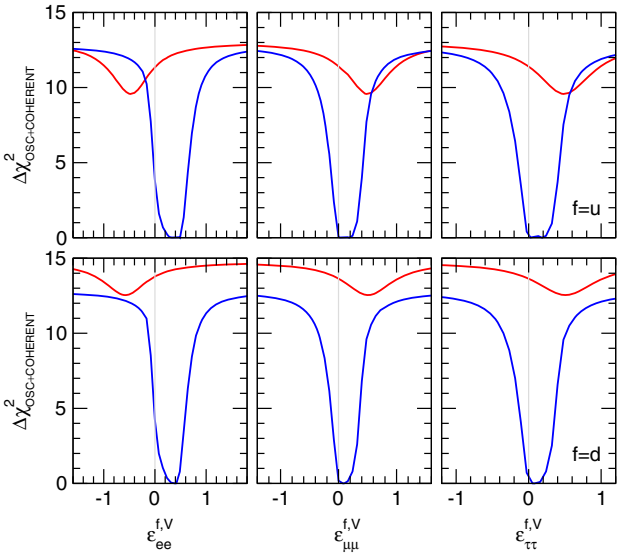

FIG. 3. Bounds on the flavor diagonal NSI parameters from the global fit to oscillation plus COHERENT data. Blue lines correspond to the LMA solution ($\theta_{12} < \pi/4$), while the red lines correspond to the LMA-D solution ($\theta_{12} > \pi/4$).

restricted to flavor diagonal NSI with $f = u$ quarks. Oscillation data only constrain the difference $\epsilon^{f,V}_{ee} - \epsilon^{f,V}_{\mu\mu}$, and therefore two separate bands in this plane are allowed by the data: one corresponding to the LMA and a second one corresponding to the LMA-D solution. Conversely, the COHERENT experiment constrains the combination given in Eq. (6), and therefore its results project onto an ellipse in this plane.

V. RESULTS

Our final results for the combined fit of oscillations and COHERENT data are given in Fig. 1, where we show as full lines the total $\Delta\chi^2 = \Delta(\chi^2_{\rm OSC} + \chi^2_{\rm COH})$ as a function of the NSI parameters $\epsilon^{f,V}_{\alpha\beta}$, for $f = u$ (upper panels) and $f = d$ (lower panels) after marginalization over the undisplayed oscillation and NSI parameters in each panel. While the LMA-D solution is perfectly compatible with oscillation data alone, we find that, once COHERENT data are included in the fit, it is disfavored with respect to LMA with $\Delta\chi^2 \geq 9.6$ (12.6) for $f = u$ ($f = d$), which corresponds to 3.1σ (3.6σ) for 1 dof.

When oscillation parameters are marginalized within the "standard" LMA region, the global analysis slightly favors nonvanishing diagonal NSI. The reason for this lies in the 2σ tension between the determination of Δm^2_{21} from KamLAND and solar neutrino experiments (see, for example, Ref. [1] for the latest status on this issue).

In order to stress the effect of COHERENT in the fit with respect to the constraints already provided by oscillation data, the results for the diagonal NSI parameters are shown in Fig. 1 for the differences $\epsilon^{f,V}_{ee} - \epsilon^{f,V}_{\mu\mu}$ and $\epsilon^{f,V}_{\tau\tau} - \epsilon^{f,V}_{\mu\mu}$, to which oscillations are sensitive. Notice, however, that the inclusion of COHERENT data allows one to set independent bounds on all $\epsilon^{f,V}_{\alpha\alpha}$, since COHERENT depends on a different combination of $\epsilon^{f,V}_{ee}$ and $\epsilon^{f,V}_{\mu\mu}$. We show the projection of the marginalized $\Delta\chi^2$ for each flavor diagonal NSI in Fig. 3. As can be seen, the combined fit of COHERENT and oscillation data is capable of constraining the individual flavor diagonal NSI up to $\Delta\chi^2 \sim 12$. Beyond that level, oscillation data dominate, and only the two differences relevant for oscillations are effectively bounded, which leads to the flattening of the marginalized $\Delta\chi^2$ as a function of the individual diagonal NSI.

The 90% C.L. allowed ranges for the NSI parameters from our global analysis are given in Table I. The addition of COHERENT data allows one to derive competitive constraints on each of the diagonal parameters separately. This is especially relevant for $\epsilon^{f,V}_{\tau\tau}$ for which the new bound $-0.09 < \epsilon^{u,V}_{\tau\tau} < 0.38$ ($-0.075 < \epsilon^{d,V}_{\tau\tau} < 0.33$) at 90% C.L. represents the first direct bound on NC vector interactions of ν_τ

TABLE I. Allowed ranges at 90% C.L. for the NSI parameters $\epsilon^{f,V}_{\alpha\beta}$ for $f = u$, d, as obtained from a global fit to oscillation and COHERENT data. The results for each NSI parameter are obtained after marginalizing over all oscillation and the other NSI parameters.

	$f = u$	$f = d$
$\epsilon^{f,V}_{ee}$	[0.028, 0.60]	[0.030, 0.55]
$\epsilon^{f,V}_{\mu\mu}$	[−0.088, 0.37]	[−0.075, 0.33]
$\epsilon^{f,V}_{\tau\tau}$	[−0.090, 0.38]	[−0.075, 0.33]
$\epsilon^{f,V}_{e\mu}$	[−0.073, 0.044]	[−0.07, 0.04]
$\epsilon^{f,V}_{e\tau}$	[−0.15, 0.13]	[−0.13, 0.12]
$\epsilon^{f,V}_{\mu\tau}$	[−0.01, 0.009]	[−0.009, 0.008]

assuming light mediators and is an order of magnitude stronger than previous indirect (loop induced) limits [28]. We also see that for $\epsilon_{ee}^{f,V}$ the 90% C.L. range does not include zero. As explained above, this "nonstandard" result is driven by the 2σ tension in the determination of $\Delta m^2{}_{21}$ from KamLAND and in solar neutrino experiments and is still consistent with COHERENT results within present precision.

VI. CONCLUSIONS

In this work, we have combined the recently reported measurement of neutrino-nucleus coherent scattering by the COHERENT Collaboration with data from neutrino oscillation experiments, in order to constrain neutrino NSI affecting NC interactions with quarks. We find that the addition of COHERENT to the global fit from oscillation data excludes the LMA-D solution at 3.1σ (3.6σ) C.L. for NSI with up (down) quarks due to the exchange of a new mediator with a mass above 10 MeV. In addition, the combination of oscillation and COHERENT data allows one to derive competitive constraints on all diagonal NSI parameters individually.

ACKNOWLEDGMENTS

This work is supported by USA-NSF Grant No. PHY-1620628; by EU Networks FP10 ITN ELUSIVES (Grant No. H2020-MSCA-ITN-2015-674896) and INVISIBLES-PLUS (Grant No. H2020-MSCA-RISE-2015-690575); by MINECO Grants No. FPA2016-76005-C2-1-P and No. FPA2012-31880 and MINECO/FEDER-UE Grants No. FPA2015-65929-P and No. FPA2016-78645-P; by Maria de Maetzu program Grant No. MDM-2014-0367 of ICCUB; and by the "Severo Ochoa" program Grant No. SEV-2016-0597 of IFT. This manuscript has been authored by Fermi Research Alliance, LLC, under Contract No. DE-AC02-07CH11359 with the U.S. Department of Energy, Office of Science, Office of High Energy Physics. The publisher, by accepting the article for publication, acknowledges that the United States Government retains a nonexclusive, paid-up, irrevocable, worldwide license to publish or reproduce the published form of this manuscript, or allow others to do so, for United States Government purposes.

[1] I. Esteban, M. C. Gonzalez-Garcia, M. Maltoni, I. Martinez-Soler, and T. Schwetz, Updated fit to three neutrino mixing: exploring the accelerator-reactor complementarity, J. High Energy Phys. 01 (2017) 087.
[2] L. Wolfenstein, Neutrino oscillations in matter, Phys. Rev. D **17**, 2369 (1978).
[3] J. W. F. Valle, Resonant oscillations of massless neutrinos in matter, Phys. Lett. B **199**, 432 (1987).
[4] M. M. Guzzo, A. Masiero, and S. T. Petcov, On the MSW effect with massless neutrinos and no mixing in the vacuum, Phys. Lett. B **260**, 154 (1991).
[5] O. G. Miranda, M. A. Tortola, and J. W. F. Valle, Are solar neutrino oscillations robust?, J. High Energy Phys. 10 (2006) 008.
[6] S. P. Mikheev and A. Y. Smirnov, Resonance enhancement of oscillations in matter and solar neutrino spectroscopy, Sov. J. Nucl. Phys. **42**, 913 (1985).
[7] M. C. Gonzalez-Garcia, M. Maltoni, and J. Salvado, Testing matter effects in propagation of atmospheric and long-baseline neutrinos, J. High Energy Phys. 05 (2011) 075.
[8] M. C. Gonzalez-Garcia and M. Maltoni, Determination of matter potential from global analysis of neutrino oscillation data, J. High Energy Phys. 09 (2013) 152.
[9] P. Bakhti and Y. Farzan, Shedding light on LMA-Dark solar neutrino solution by medium baseline reactor experiments: JUNO and RENO-50, J. High Energy Phys. 07 (2014) 064.
[10] P. Coloma and T. Schwetz, Generalized mass ordering degeneracy in neutrino oscillation experiments, Phys. Rev. D **94**, 055005 (2016).
[11] P. Coloma, P. B. Denton, M. C. Gonzalez-Garcia, M. Maltoni, and T. Schwetz, Curtailing the dark side in non-standard neutrino interactions, J. High Energy Phys. 04 (2017) 116.
[12] F. J. Escrihuela, O. G. Miranda, M. A. Tortola, and J. W. F. Valle, Constraining nonstandard neutrino-quark interactions with solar, reactor and accelerator data, Phys. Rev. D **80**, 105009 (2009).
[13] D. Z. Freedman, Coherent neutrino nucleus scattering as a probe of the weak neutral current, Phys. Rev. D **9**, 1389 (1974).
[14] D. Akimov *et al.*, Observation of coherent elastic neutrino-nucleus scattering, Science **357**, 1123 (2017).
[15] J. Barranco, O. G. Miranda, and T. I. Rashba, Probing new physics with coherent neutrino scattering off nuclei, J. High Energy Phys. 12 (2005) 021.
[16] K. Scholberg, Prospects for measuring coherent neutrino-nucleus elastic scattering at a stopped-pion neutrino source, Phys. Rev. D **73**, 033005 (2006).
[17] B. Dutta, R. Mahapatra, L. E. Strigari, and J. W. Walker, Sensitivity to Z-prime and nonstandard neutrino interactions from ultralow threshold neutrino-nucleus coherent scattering, Phys. Rev. D **93**, 013015 (2016).
[18] M. Lindner, W. Rodejohann, and X.-J. Xu, Coherent neutrino-nucleus scattering and new neutrino interactions, J. High Energy Phys. 03 (2017) 097.
[19] I. M. Shoemaker, COHERENT search strategy for beyond standard model neutrino interactions, Phys. Rev. D **95**, 115028 (2017).

[20] M. B. Gavela, D. Hernandez, T. Ota, and W. Winter, Large gauge invariant non-standard neutrino interactions, Phys. Rev. D **79**, 013007 (2009).

[21] S. Antusch, J. P. Baumann, and E. Fernandez-Martinez, Non-standard neutrino interactions with matter from physics beyond the standard model, Nucl. Phys. **B810**, 369 (2009).

[22] Y. Farzan, A model for large non-standard interactions of neutrinos leading to the LMA-Dark solution, Phys. Lett. B **748**, 311 (2015).

[23] Y. Farzan and I. M. Shoemaker, Lepton flavor violating non-standard interactions via light mediators, J. High Energy Phys. 07 (2016) 033.

[24] K. S. Babu, A. Friedland, P. A. N. Machado, and I. Mocioiu, Flavor gauge models below the Fermi scale, arXiv: 1705.01822.

[25] O. G. Miranda and H. Nunokawa, Non standard neutrino interactions: current status and future prospects, New J. Phys. **17**, 095002 (2015).

[26] J. Dorenbosch *et al.* (CHARM Collaboration), Experimental verification of the universality of ν_e and ν_μ coupling to the neutral weak current, Phys. Lett. B **180**, 303 (1986).

[27] G. P. Zeller *et al.* (NuTeV Collaboration), A Precise Determination of Electroweak Parameters in Neutrino Nucleon Scattering, Phys. Rev. Lett. **88**, 091802 (2002).

[28] S. Davidson, C. Pena-Garay, N. Rius, and A. Santamaria, Present and future bounds on nonstandard neutrino interactions, J. High Energy Phys. 03 (2003) 011.